Soil Moisture Active Passive (SMAP) Project
Radar Backscatter Calibration for the L1B_S0_LoRes and L1C_S0_HiRes Beta Level Data Products

Prepared by:

Richard West
SMAP Radar Instrument Scientist

8/5/2015
Date

Approved by:

Michael Spencer
SMAP Cal/Val Lead

8/5/2015
Date

Simon Yueh
SMAP Project Scientist

8/6/2015
Date

Paper copies of this document may not be current and should not be relied on for official purposes. The current version is in the Product Data Management System (PDMS): https://pdms.jpl.nasa.gov/

July 30, 2015
D-93979

Jet Propulsion Laboratory
California Institute of Technology

Copyright 2015 California Institute of Technology. U.S. Government sponsorship acknowledged.

DOCUMENT CHANGE LOG

Revision	Date	Sections Changed	Reason for Change

Copyright 2015 California Institute of Technology. U.S. Government sponsorship acknowledged.

TBD, TBR, TBS LOG

Section/Page	Description	Due Date

Copyright 2015 California Institute of Technology. U.S. Government sponsorship acknowledged.

Copyright 2015 California Institute of Technology. U.S. Government sponsorship acknowledged.

Executive Summary

This report provides analysis and assessment of calibration quality of SMAP radar normalized backscatter cross-section (σ_0) for the L1B_S0_LoRes and L1C_S0_HiRes beta-level data products. The primary radiometric calibration methods are: 1) comparison against the stable regions of the Amazon previously measured by PALSAR and Aquarius, and 2) Comparison of the ocean wind speed model function derived from SMAP data to that derived from Aquarius data. Geo-location is verified using the location of known landmarks, such as coastlines, as well as the known location of large radar corner reflectors located in the California desert. It was found that the "out of the box" absolute bias of measurements relative to PALSAR and Aquarius is remarkably small: less than 1 dB for the co-pol measurements, and also on that order for the cross-pol measurements. Another key calibration task is to ensure that σ_0 measurements are free from any swath location dependent biases – that is, if the scene over the 1000 km radar swath is constant, the retrieved σ_0's should also be constant. This analysis is again performed using both the Amazon and ocean measurements.

A summary of the quality and features of the beta released data is as follows:

- Calibration Relative to PALSAR and Aquarius: The SMAP co-pol measurements are in agreement to better than 1 dB. The cross-pol measurements agree to order 1 dB. (These residual biases should be reduced to less than 0.2 dB in the later Validated Data Release.)

- Across Swath Biases: For both the L1B_S0_LoRes and L1C_S0_HiRes data, relative biases across most of the swath are less than 0.3 dB. For the L1C_S0_HiRes there is a residual pronounced bias near the nadir track. This bias, however, is in the region indicated by the "nadir flag" where the product may not meet all radiometric performance requirements anyway. (Nevertheless, the objective for the ultimate Validated Release is to remove this near nadir artifact.)

- Faraday Rotation Correction: In the beta release, the L1B_S0_LoRes product has the Faraday rotation correction turned "on" whereas in the L1C_S0_HiRes product has the Faraday rotation correction turned "off." This consequently results in somewhat better cross-pol performance for the LoRes data, particularly over regions where the cross-pol to co-pol ratio is low. (The Faraday rotation will be fully operational for the HiRes at the time of the Validated Release.)

The detailed sections of this report note several other limitations and unaddressed areas in the beta-level calibration. Despite this remaining work, the beta-level product is of sufficient quality that it should be distributed to and used by the larger science and application communities.

1 Introduction

The SMAP radar was designed to provide global radar backscatter measurements (sigma0) with a three day revisit time. The high resolution L1C radar product contains measurements posted on a 1-km swath grid. The swath grid follows the orbit path, and data are divided into half-orbit granules. L1 Radar processing was specified to provide these half-orbit products within 12 hours of acquisition. During the cal/val period, the average latency was about 9 hours. The relative accuracy requirement for co-pol radar backscatter is 1 dB overall, and 0.4 dB for calibration errors. The beta product is not guaranteed to meet this requirement, however, as discussed below, the residual relative calibration errors appear to be less than 1 dB for the co-pol channels. Cross-pol errors are higher in part due to the absence of Faraday rotation corrections in the high-res data. These uncertainties will be reduced in the validated release. Figure 1 shows a global composite of high-res radar data taken from several days of half-orbit products. These data are color scaled according to the polarization of the data. The SMAP radar captures two co-pol channels (HH and VV) and one cross-pol channel (HV). (RFI mitigation was not activated for this particular image, so some green spots are visible which are due to strong RFI signals.) In the following sections, we describe in more detail different aspects of the beta data release. More information can be obtained from the following documents available on the SMAP website: smap.jpl.nasa.gov.

SMAP Handbook JPL 400-1567 07/14
L1B&C Algorithm Theoretical Basis Document (ATBD) JPL-D-53052
L1B Product Specification JPL-D-72544
L1C Product Specification JPL-D-72554

Product specification documents will also be available along with the beta release data from the Alaska Sar Facility (ASF) at: www.asf.alaska.edu.

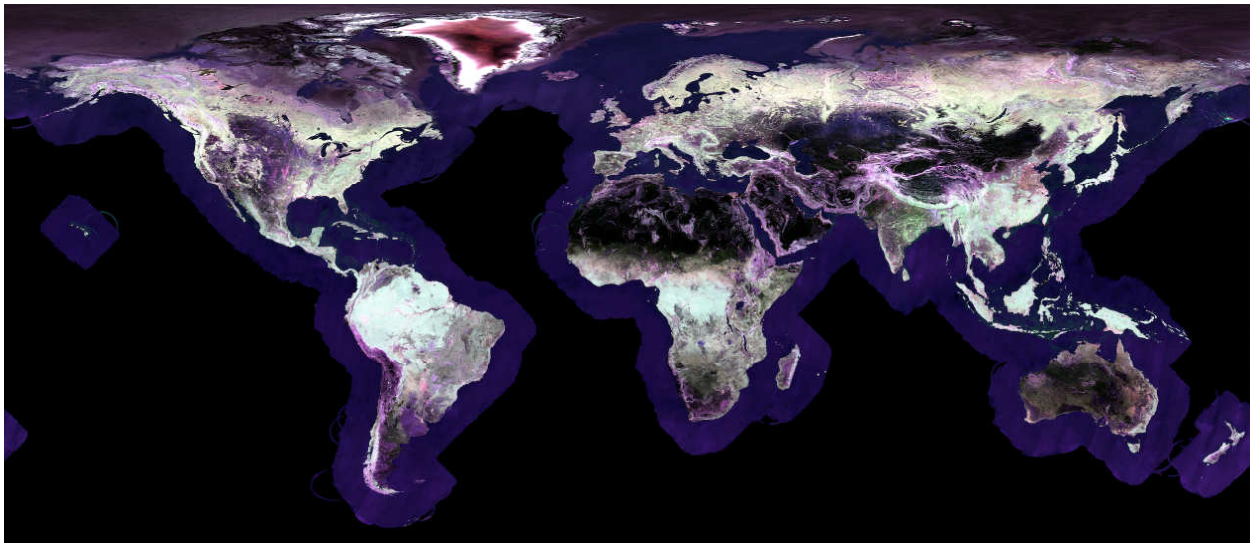

Figure 1: Global view of polarimetric L1C data.

2 Details Sections

High-Resolution Coverage

The SMAP radar collects both high- and low-resolution data. The low-resolution data are collected whenever radar transmit is enabled. Since transmit is nearly continuous, global low-resolution data over both land and ocean areas, including Antarctica, are available in the L1B_S0_LoRes product. High-resolution data are collected as specified in an 8-day instrument Look Up Table (LUT). Several LUT versions have been used since the initial epoch of the released data. This was needed as each LUT increases the data volume, and the Mission System needed to verify end-to-end data downlink and processing capabilities gradually as data volume increased.
The Table below specifies the changes in LUT and their activation dates and orbits.

Date	Time	DOY	Orbit #	Description
4/13/15	18:39	103	1056_A	Activated ALT1 Science LUT, frequency index 9
4/16/15	20:39	106	1101_D	Activated Timing Test LUT, index 9
4/17/15	20:28	107	1116_A	Re-activated ALT1 Science LUT, index 9
4/22/15	22:25	112	1190_A	Re-activated Timing Test LUT, index 9
4/24/15	16:26	114	1215_D	Activated ALT1 Science LUT, frequency index 5
4/29/15	17:13	119	1289_D	Activated North & South America LUT, index 5
5/4/15	21:04	124	1365_A	Activated All Land LUT, index 5
7/7/15	17:00	188	2298_D	Activate Atlantic Hurricane LUT, index 5

(Note, there is an 8 minute period prior to the LUT activation time when LUT operations is suspended and data may be degraded.)

The LUT characteristics may be summarized as follows:

1. ALT 1 Science LUT, frequency index 9: In the ALT1 LUT (figure below), Arctic areas (blue-green) are imaged in high-res on both ascending and descending passes, both forward and aft looking. Other land areas (gold) are imaged forward and aft only in descending passes. The near-coastal oceans (red) are imaged only forward-looking in descending passes. This LUT uses frequency index 9 (1230.0 MHz center frequency).

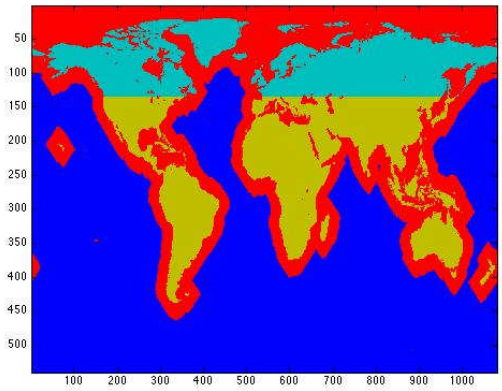

2. Timing Test LUT: The Timing Test LUT (figure below) was a special LUT for Instrument Commissioning, where hi-res and low-res data were interspersed around the globe. Fifty scans (4.11 sec each) of high-res data (blue) were followed by 100 scans of low-res data (red). Data coverage is approximately as shown for the descending arcs, and there is similar coverage for the ascending arcs.

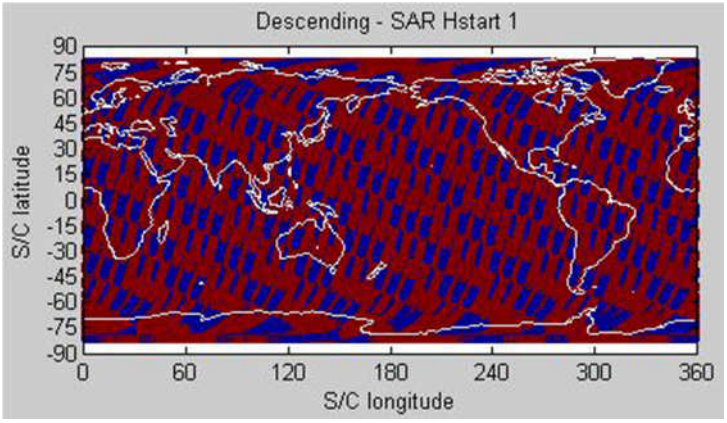

3. ALT 1 Science LUT, frequency index 5: This LUT (not shown) has coverage identical to the ALT1 LUT at index 9, but now frequency index 5 is used (center frequency = 1225.0 MHz) for reduced impact from radio frequency interference (RFI).

4. North and South America LUT: This LUT (see figure below) included high-res coverage of all North and South America, both ascending and descending arcs, fore and aft looking. It used frequency index 5.

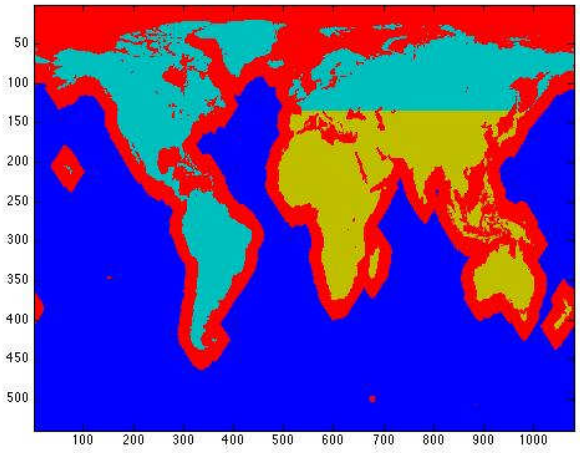

5. All Land LUT: In this LUT (see below), all land areas are imaged in hi-resolution, both ascending and descending and foreward and aft. Near-coastal oceans are still imaged in descending orbits only, and forward-looking only. The frequency index remains 5.

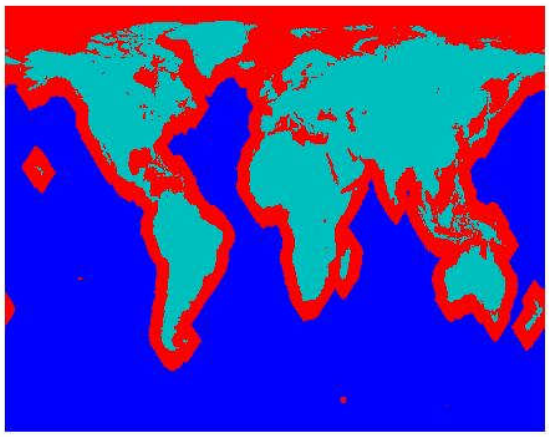

6. Atlantic Hurricane LUT: This LUT (see below) was in use, unfortunately, for only 4 hours before transmitting ceased. It added high-res data (fore and aft, ascending and descending) over the Northern Atlantic ocean in the primary hurricane forming

regions (green).

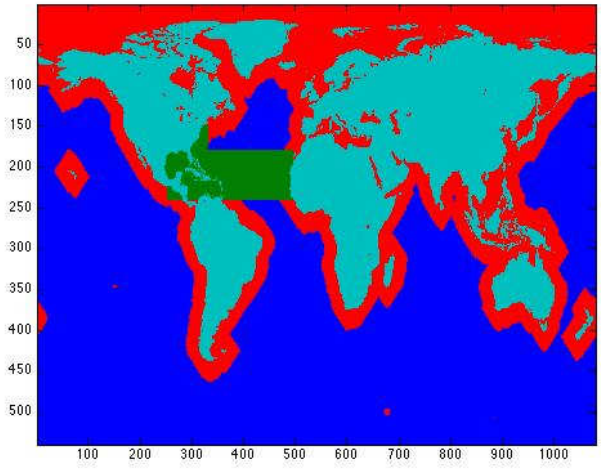

The high-resolution radar data acquisition is designed to provide coverage every 3 days if the nadir region is included, and every 8 days if the nadir region is excluded. The nadir region is the middle 300 km of the swath where the observation geometry may not allow measurements that meet requirements for all applications. The next four figures show the low-resolution (L1B) radar coverage from 3 days of data. Then the following 6 figures show the high-resolution (L1C) radar coverage from 8 days of data while excluding the nadir region. High-resolution data separates fore and aft measurements which are shown separately. In these figures, we see complete high-resolution land coverage for the aft measurements in 8 days, and complete land coverage with extra coastal ocean coverage for the forward measurements. The low-resolution radar data provide complete global coverage including the oceans every 3 days.

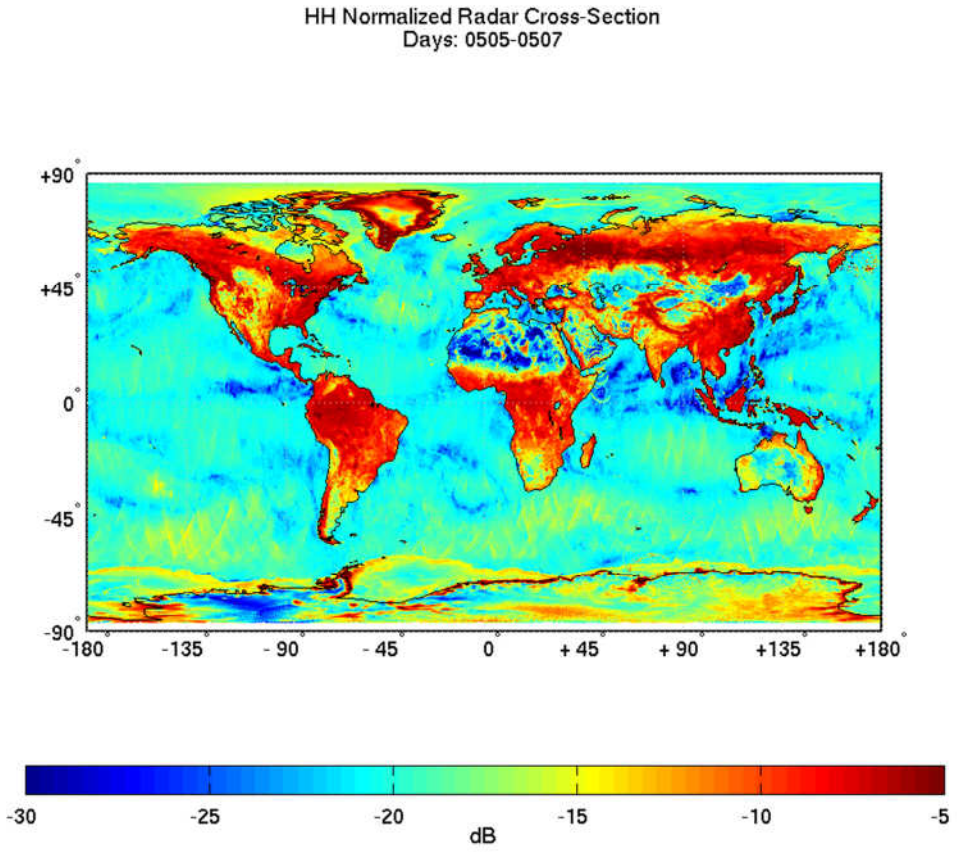

Co-pol horizontally polarized low-resolution backscatter composite from 3 days of data. Low-resolution measurements cover the entire globe.

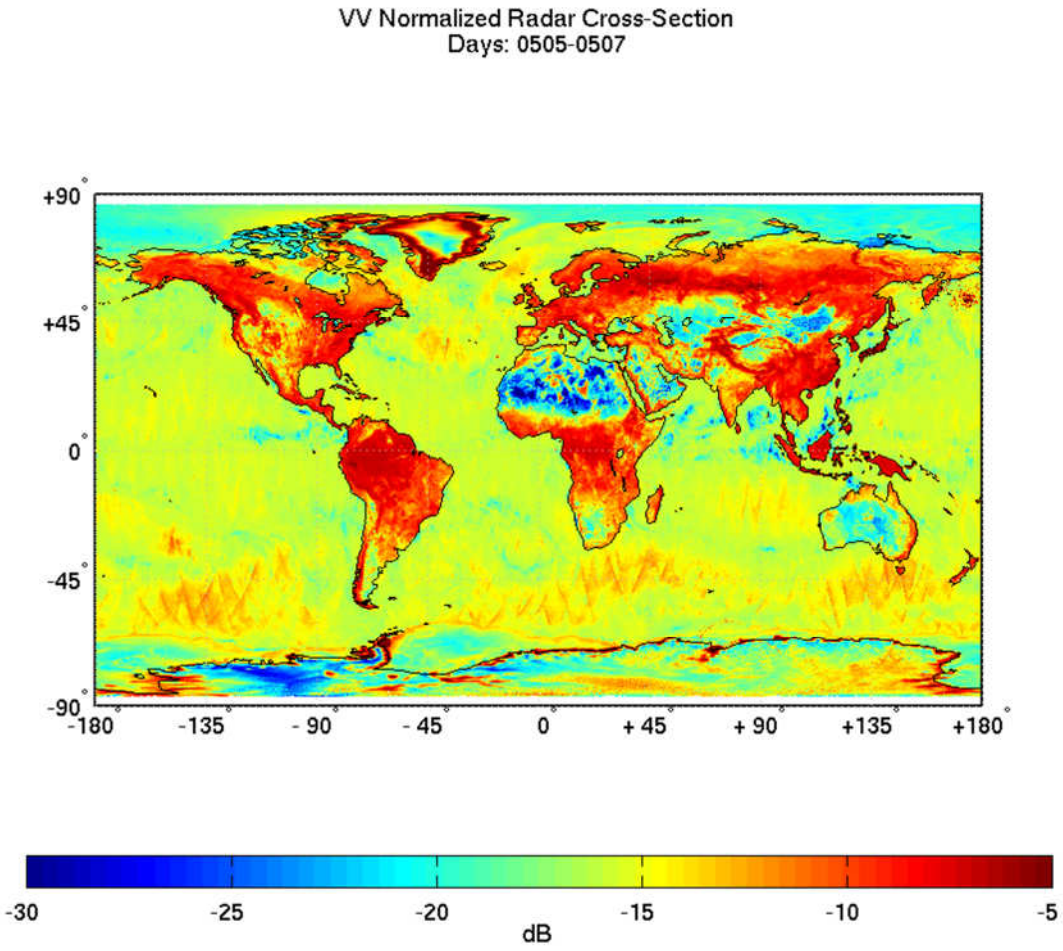

Co-pol vertically polarized low-resolution backscatter composite from 3 days of data. Low-resolution measurements cover the entire globe.

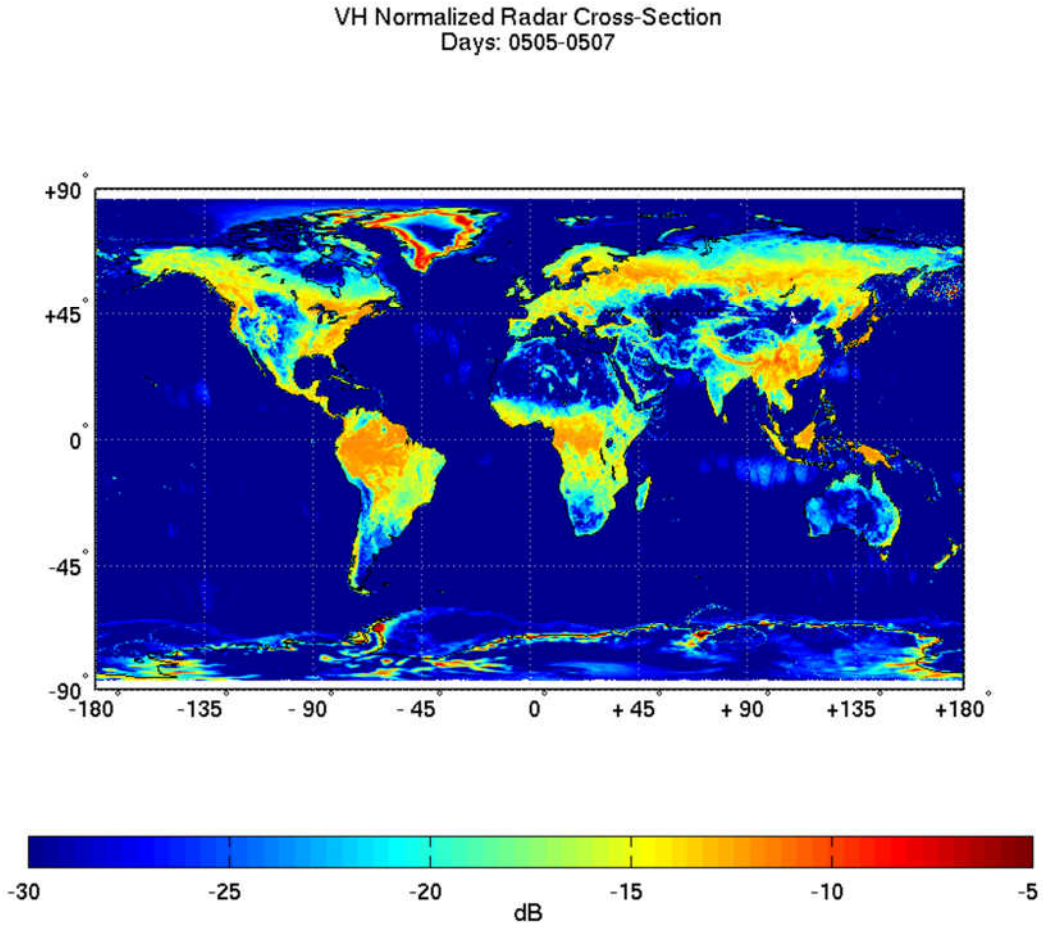

Cross-pol (VH) low-resolution backscatter composite from 3 days of data. Low-resolution measurements cover the entire globe.

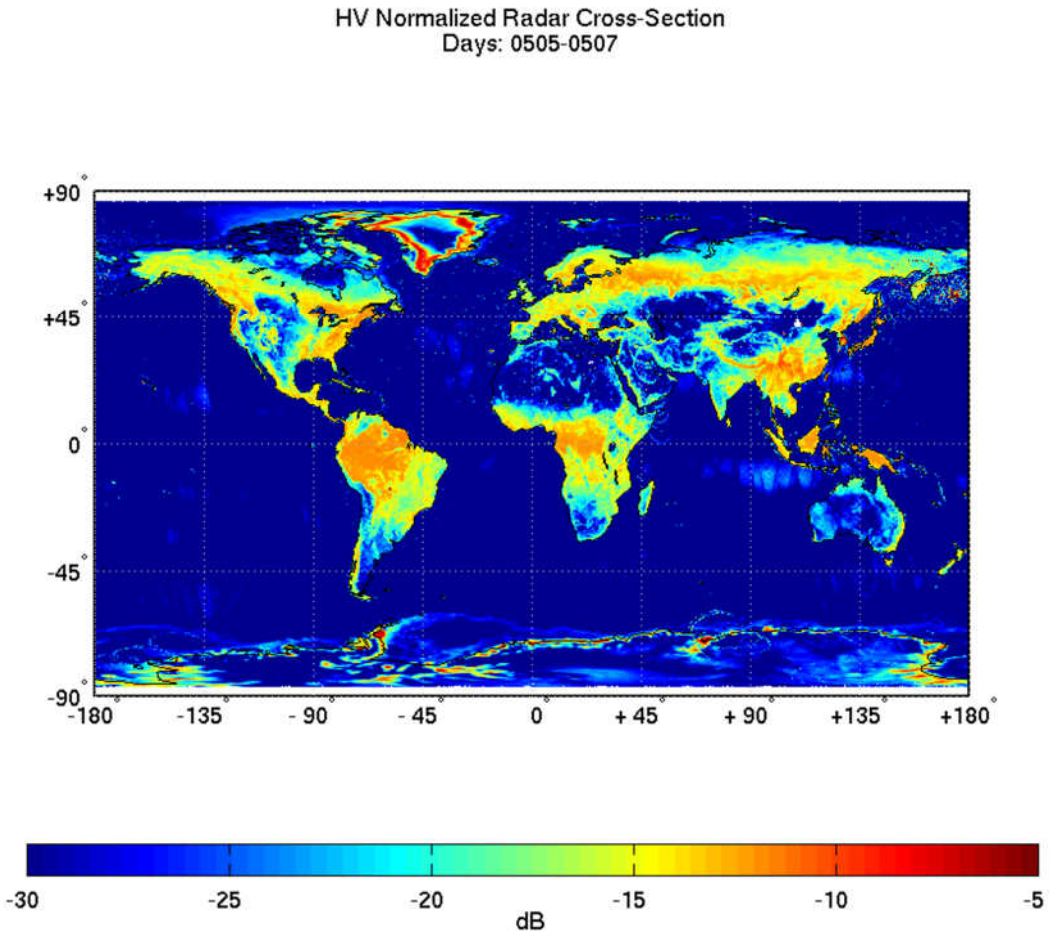

Cross-pol (HV) low-resolution backscatter composite from 3 days of data. Low-resolution measurements cover the entire globe.

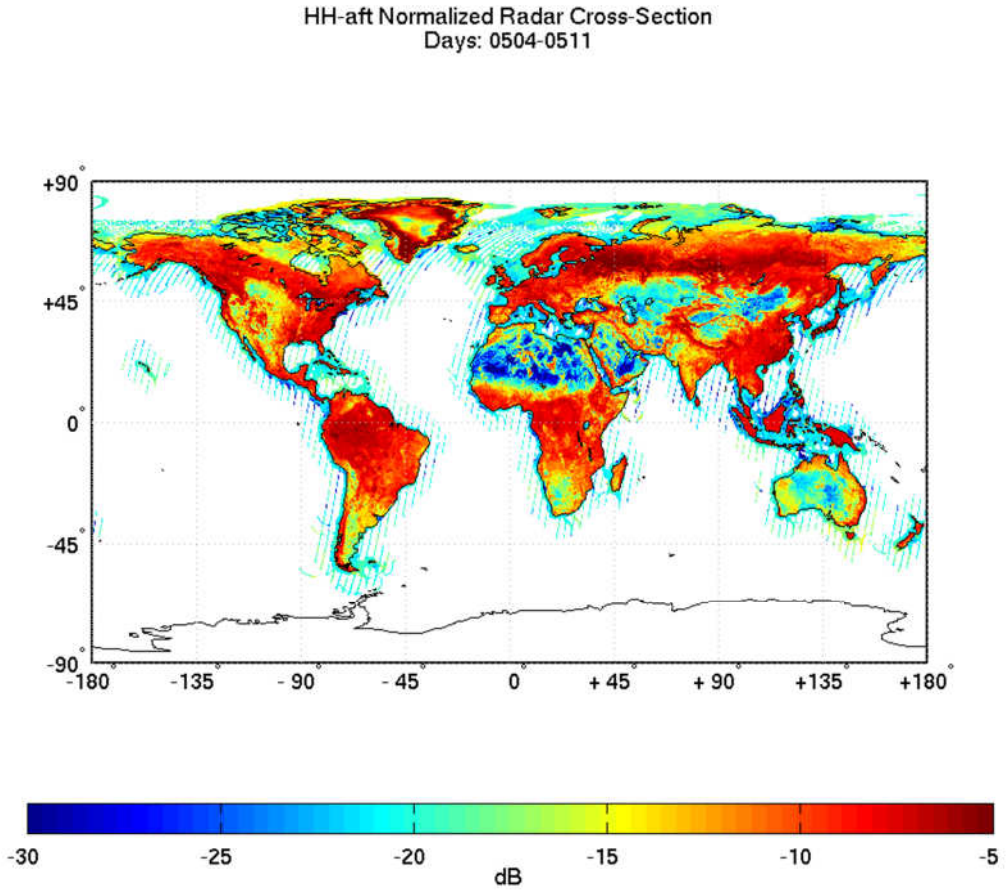

Co-pol horizontal polarization high-resolution backscatter composite from 8 days, excluding the nadir region measurements. Aft looks include land only.

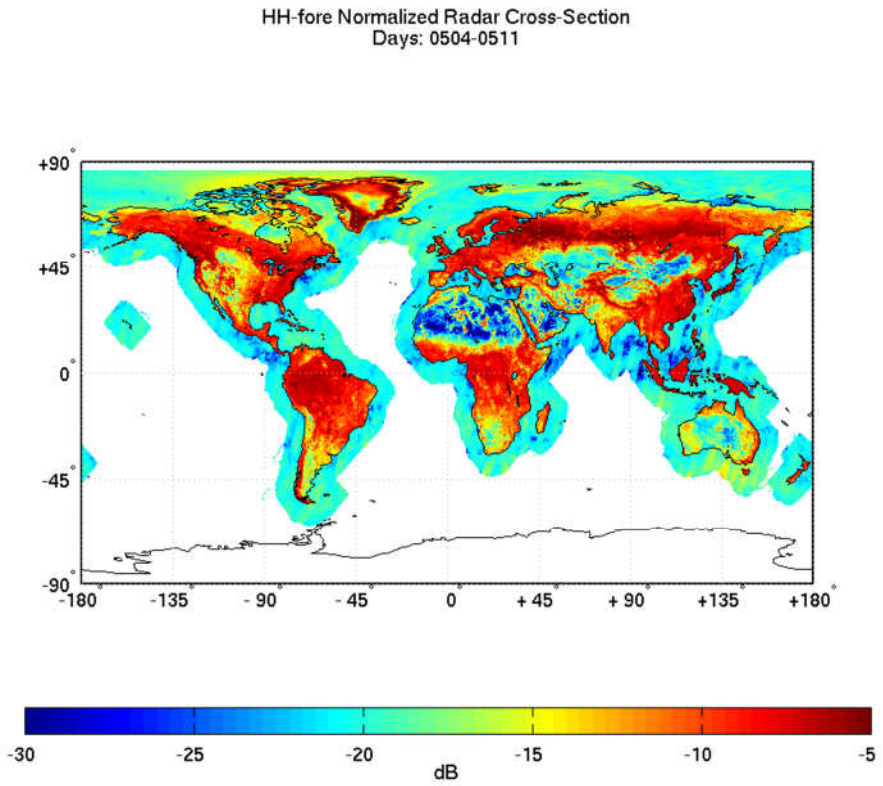

Co-pol horizontal polarization high-resolution backscatter composite from 8 days, excluding the nadir region measurements. Forward looks include coastal ocean.

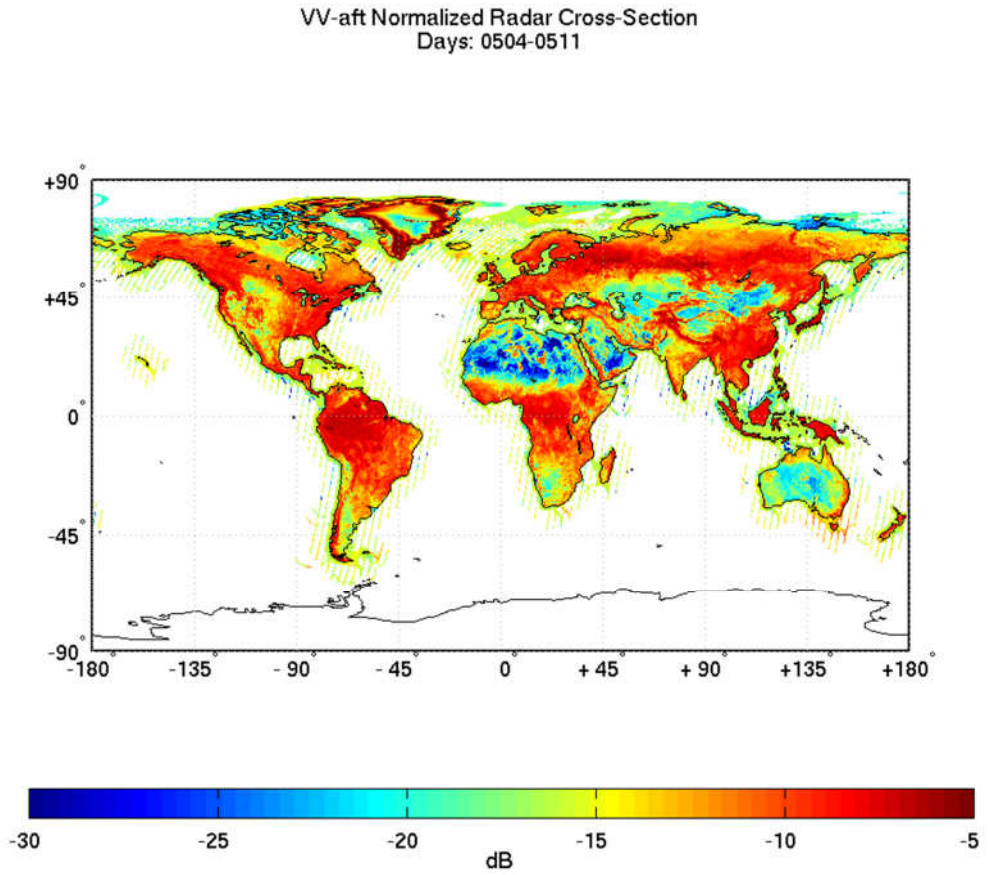

Co-pol vertical polarization high-resolution backscatter composite from 8 days, excluding the nadir region measurements. Aft looks include land only.

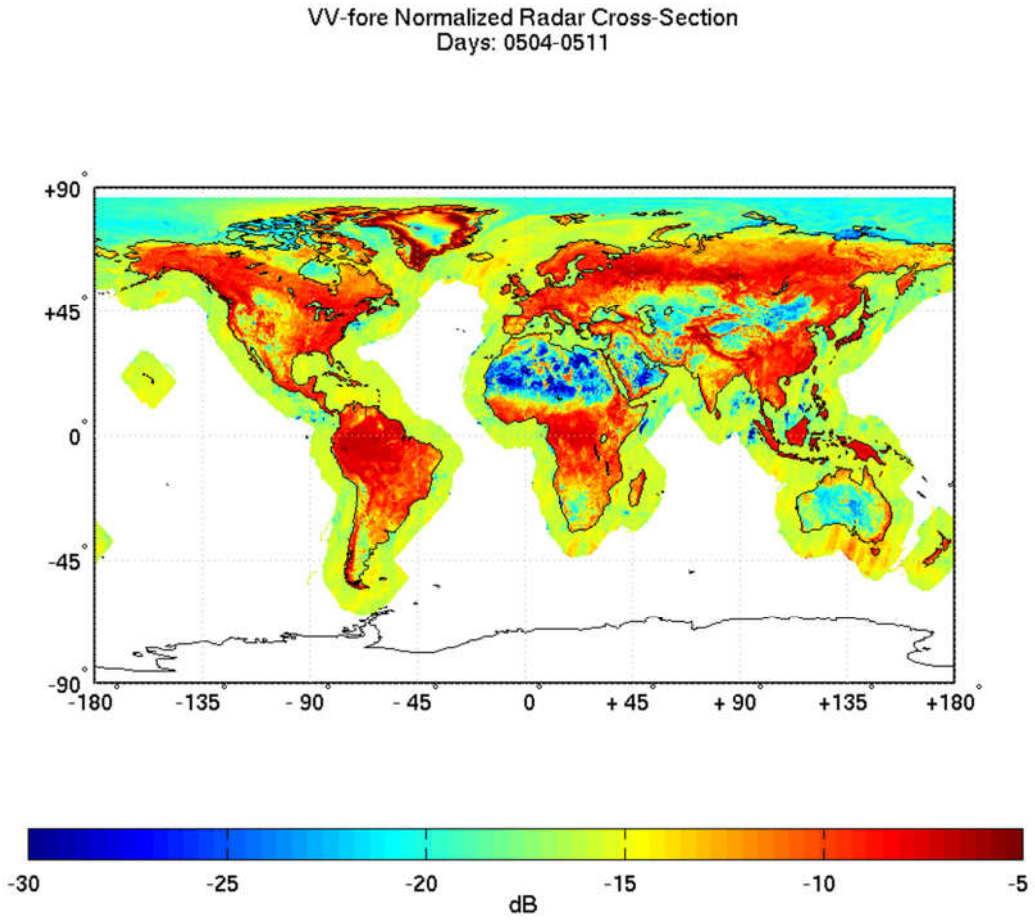

Co-pol vertical polarization high-resolution backscatter composite from 8 days, excluding the nadir region measurements. Forward looks include coastal ocean.

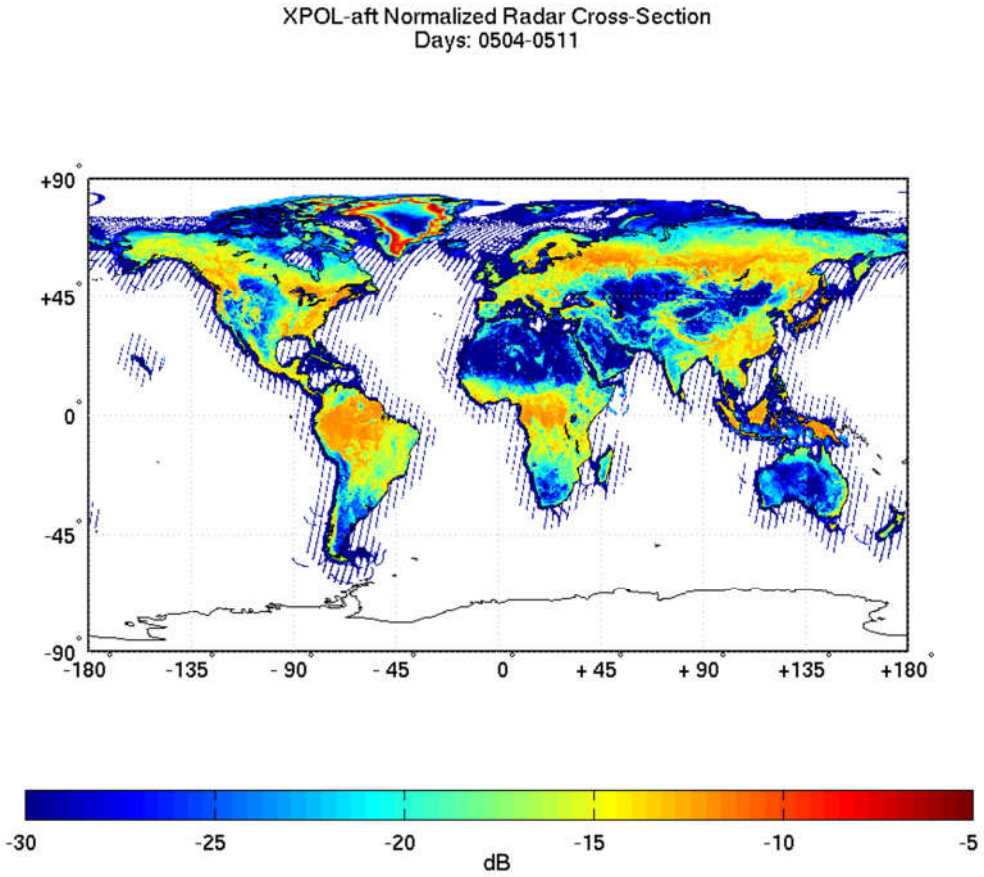

Cross-pol high-res backscatter composite from 8 days, excluding the nadir region measurements. Aft looks include land only.

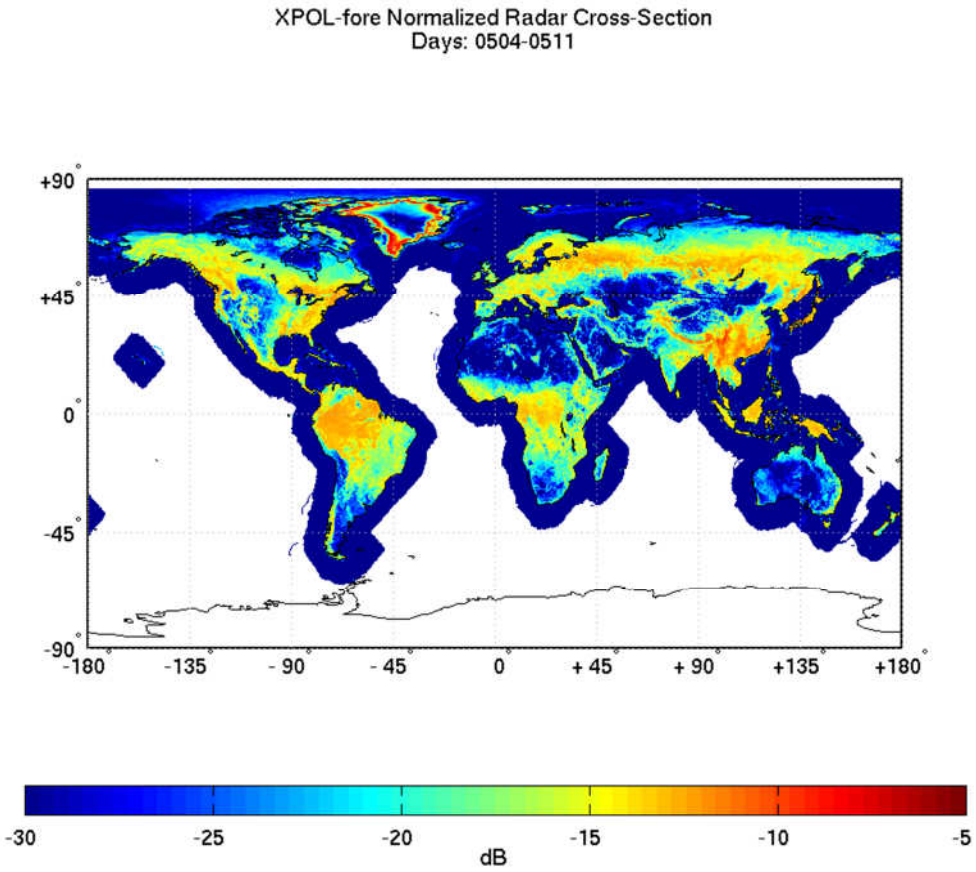

Cross-pol high-resolution backscatter composite from 8 days, excluding the nadir region measurements. Forward looks include coastal ocean.

Backscatter geo-location

The L1C_S0_HiRes products contain backscatter measurements (sigma0) posted on a 1-km spaced swath grid. The processor focuses the image directly onto the swath grid according to the range and Doppler shifts that associated with each grid point. The geodetic latitude and longitude corresponding to each grid point are also supplied at 1 km resolution. The geo-location accuracy is evaluated by plotting sigma0 using reported latitude and longitude and overlay on Google earth images and coastline information provided by the Global Self-consistent, Hierarchical, High-resolution Geography Database (GSHHG), which is publicly available and provided by the University of Hawaii. An example of such a plot is shown in Figure 2-1. Furthermore, a separate analysis product is used that is posted at 250 m resolution to investigate the finer details of geo-location matches. The results are illustrated in Figure 2-2. This shows that the backscatter geo-location matches well with known coastlines. The same analysis product is also used to check against P-band corner reflectors deployed in the Rosamond area. At this level of resolution it is observed that a systematic shift of backscatter geolocation in the order of 350 meters exists.

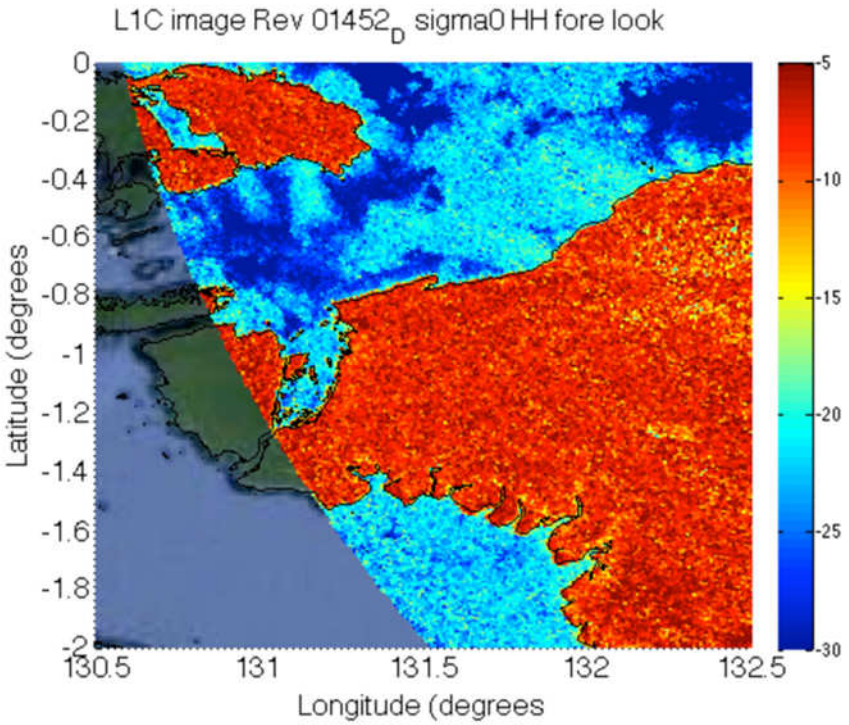

Figure 2-1: Co-location with coastlines using the L1C radar 1 km product showing good agreement of outline of backscatter with the coast line.

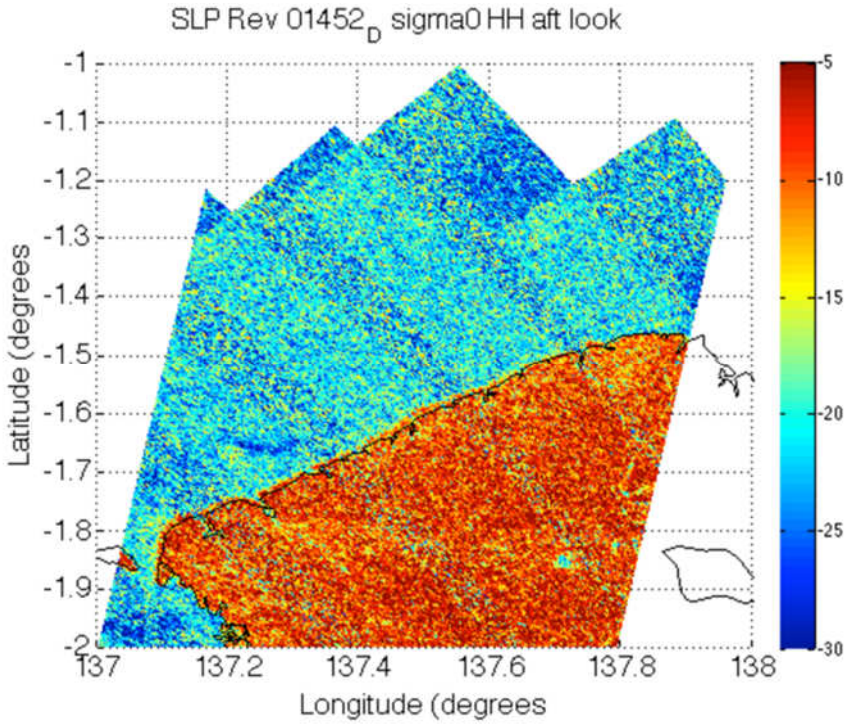

Figure 2-2: Co-location with coastlines using the 250 m analysis product.

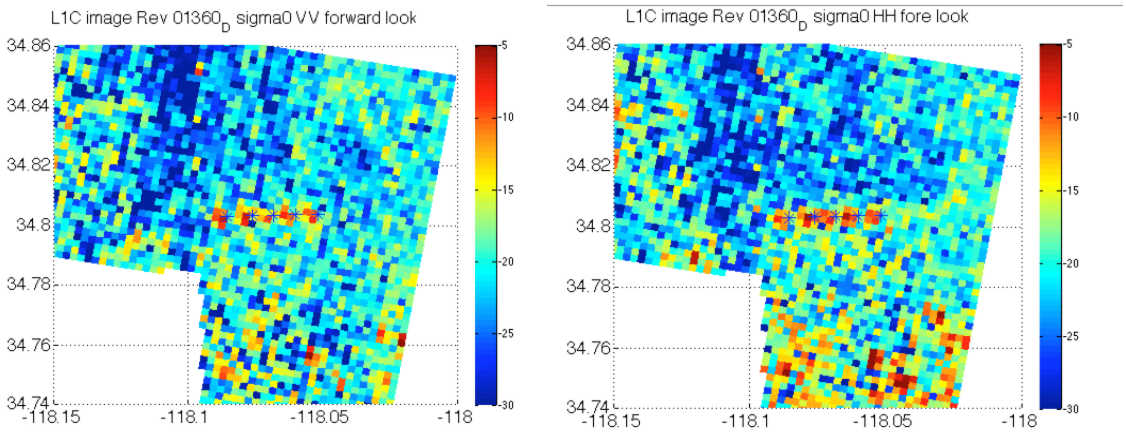

Figure 2-3: Co-location with P-band corner reflector using the 250 m analysis product. The asterisk symbols show the known exact location of the corner reflectors.

The geo-location of L1B low-resolution data is also analyzed. Because of its low-resolution nature, the geo-location cannot be done better than about 5 km. This is shown with the L1B low-resolution radar data by plotting an image of Madagascar (Figure 2-4) and observing the backscatter outline compared to the GSHHG coastline.

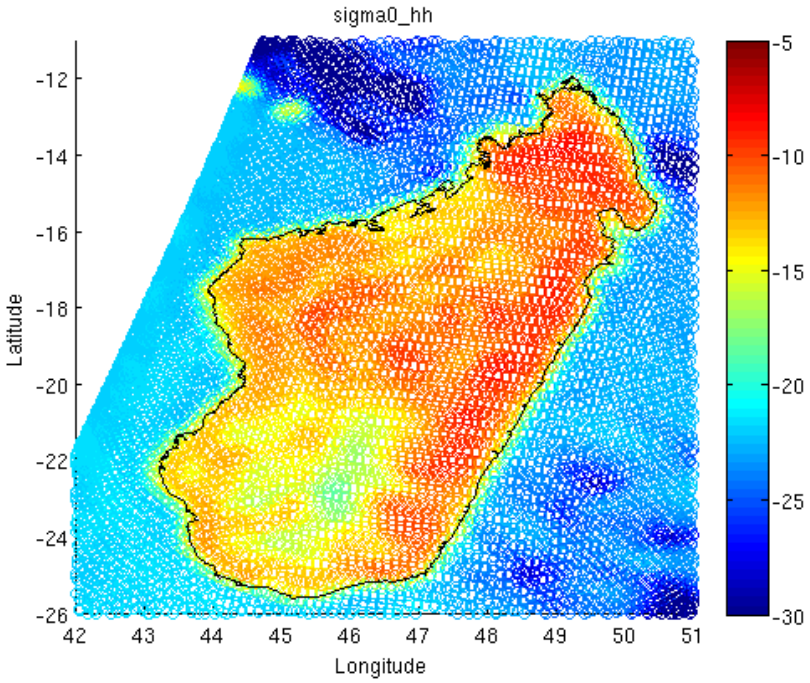

Figure 2-4: L1B geo-location. Results are good to within the resolution limit.

Image Quality

In the standard L1C product, single looks are averaged down to the output product resolution of 1 km, where it is difficult to see the underlying image quality. The SAR processor can output an analysis product at 250 m posting which we have used to examine image quality in finer detail. Figure 2-5 shows such a 250 m analysis product image for the San Francisco Bay area. The image data come from an early descending half-orbit and show a properly focused SAR image. The resolution of fine urban details such as bridges and roads is qualitatively as expected. Radar ambiguities also appear to be well controlled. Point like targets (shipping) in the Bay show some side-lobes in the point spread function that can be reduced by data windowing. Such fine-tuning of image quality may be performed before the final data release.

The SMAP L1 Radar SAR processor uses a rectangular algorithm and time domain azimuth processing which is expected to fully realize the resolution and dynamic range inherent in the data. Single look projected range resolution is fixed by the transmitted chirp bandwidth at 233 m. Single look azimuth resolution varies around the conical scan from about 360 m when side-looking down to about 1.1 km when 150 km from the nadir track. Approaching the nadir track, azimuth resolution drops to the dimensions of the beam-width as the iso-range and iso-doppler directions become parallel to each other. This range-Doppler singularity also leads to larger than desired errors in the current resolution cell area calculation, which in turn causes a near-nadir scaling artifact that is visible in images made from the SAR products. The final validated release will address this issue with an improved resolution cell area calculation in the vicinity of the nadir track.

Figure 2-5: Focusing and ambiguity performance appear nominal in 250 m analysis products. Example above shows San Francisco Bay area.

Overall Radiometric Bias

Amazon analysis

Radiometric accuracy is assessed over Amazon areas that show time stability and good homogeneity. The area used in this analysis is a one-degree box centered at -6.274 latitude,

-71.4 longitude. Backscatter data used is between data dates of April 24 to May 9. The radar backscatter data that are in this area during this data time are averaged and compared with April 2013 Aquarius data from the same area. The average backscatter in dB is shown in Figure 2-6. The L1B low-resolution radar measurements with and without Faraday rotation correction data are also processed the same way. In the table, L1B-FRon denotes the L1B data with Faraday rotation correction activated. The conclusion is that L1B low-resolution data, L1C high-resolution data and Aquarius data match very well in the co-pol (within 0.15 dB) and also match well in cross-pol (within 0.4 dB). These results are obtained using a-priori calibration constants measured by the radar system engineering group before launch. No post-launch absolute corrections are applied in the beta products (but will be in the Validated Release).

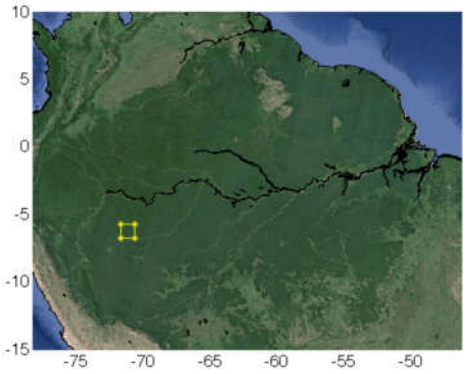

	HH asc	HH des	VV asc	VV des	HV asc	HV des	VH asc	VH des
AQ	-7.33	-7.41	-7.38	-7.47	-12.27	-12.38	-12.27	-12.37
L1B	-7.27	-7.27	-7.44	-7.25	-11.95	-12.20	-12.08	-11.91
L1B-FRon	-7.23	-7.27	-7.39	-7.24	-12.09	-12.21	-12.22	-11.92
L1C	-7.43	-7.24	-7.53	-7.36	-12.11	-12.25	N/A	N/A

Figure 2-6: Calibration analysis comparing Amazon backscatter level (dB) for Radar L1B, L1C data and Aquarius data.

Ocean analysis

Another check on the radiometric calibration is the comparison of observed backscatter and modeled backscatter from the ocean. From prior knowledge of the Aquarius model function, we can predict the level of backscatter from the ocean wind speed, direction and significant wave height. Based on ancillary data on wind speed, direction and significant wave height during the data acquisition time, comparisons were performed of predicted (or modeled) backscatter and the observed backscatter on the ocean using L1B low-

resolution data. The results are illustrated in Figure 2-7 below. The main conclusion is that Co-pol L1B measurements agree with the Aquarius model function to within about 1 dB. The observed cross-polarization discrepancy is higher than expected. However, this does not take into account possible Faraday rotation contamination, which is more pronounced in cross-polarization. The result in figure 2-8 demonstrate the effects of Faraday rotation. It shows that, with the data that is expected to have low Faraday rotation contamination, the observed and modeled data match extremely well, even for cross polarization. This is further confirmed by comparing L1B data that has Faraday correction with the modeled data shown in Figure 2-9. With Faraday correction, the observed data, even without filtering of low Faraday rotation contamination, show a close match with the modeled backscatter. The improvement is significant at low wind conditions.

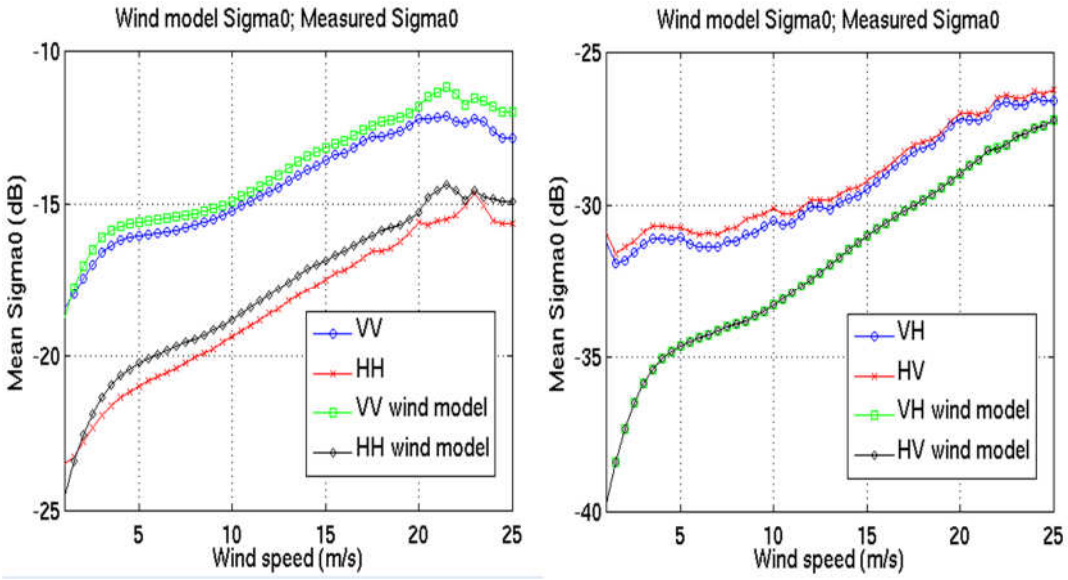

Figure 2-7: Comparison of L1B backscatter of the ocean as a function of the wind speed between observation and model. Left: the co-polarization, right: the cross-polarization. Cross-polarization measurements show the effects of uncorrected Faraday rotation.

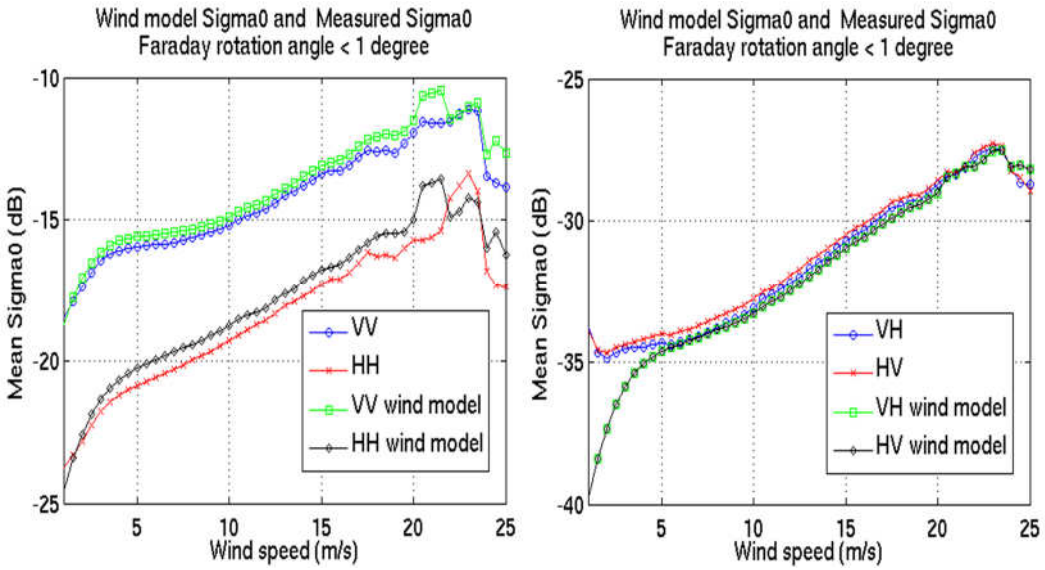

Figure 2-8: Comparison of L1B backscatter of the ocean as a function of the wind speed between observation and model. Left: the co-polarization, right: the cross-polarization. Here the measurements are filtered for Faraday rotation angles less than 1 degree. The Faraday rotation angle is obtained from ancillary total electron content measurements based on GPS data. The matchup between radar backscatter measurements and the Aquarius model function is very good when Faraday rotation is negligible.

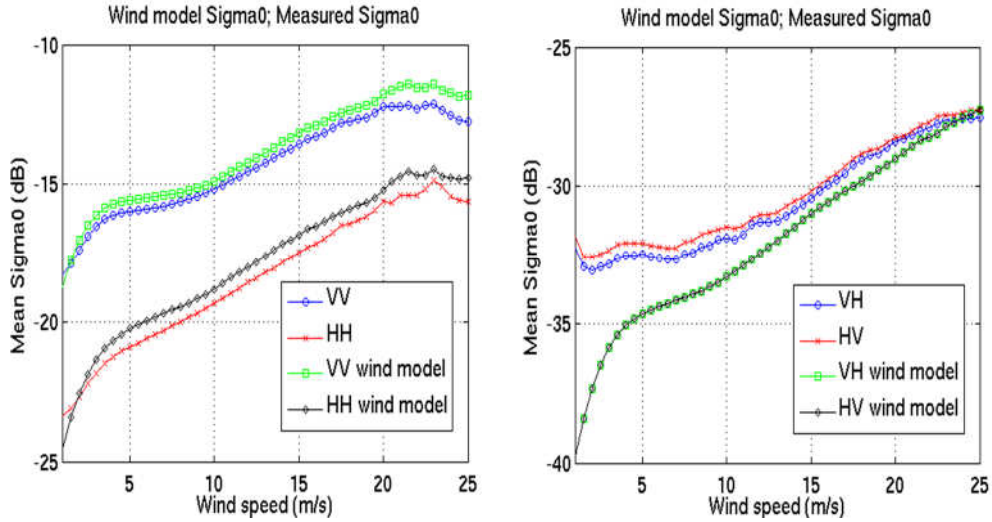

Figure 2-9: Comparison of L1B backscatter of the ocean as a function of the wind speed between observation and model. Left: the co-polarization, right: the cross-

polarization. Here a correction for Faraday rotation has been applied that improves agreement with the Aquarius model function.

Noise Subtraction

As is common with scatterometer missions, in order to produce un-biased measurements of sigma0, the background thermal noise component is detected separately and subtracted from the detected power. In order to evaluate the performance of the noise subtraction algorithm we examined one half-orbit during the RFI survey period. During this period the radar was in receive only mode and therefore the normalized cross section in the L1B and L1C product represent ambient noise equivalent sigma0. Histograms of normalized cross section from half-orbit 1049_D (04/13/2015) with noise subtraction (Figure 2-10: left) and without noise subtraction applied (Figure 2-10: right) were generated from the L1C product. Figure 2-11 shows the same thing for L1B products. This set of results shows that the noise subtraction algorithm produces noise equivalent sigma0 with mean zero as expected.

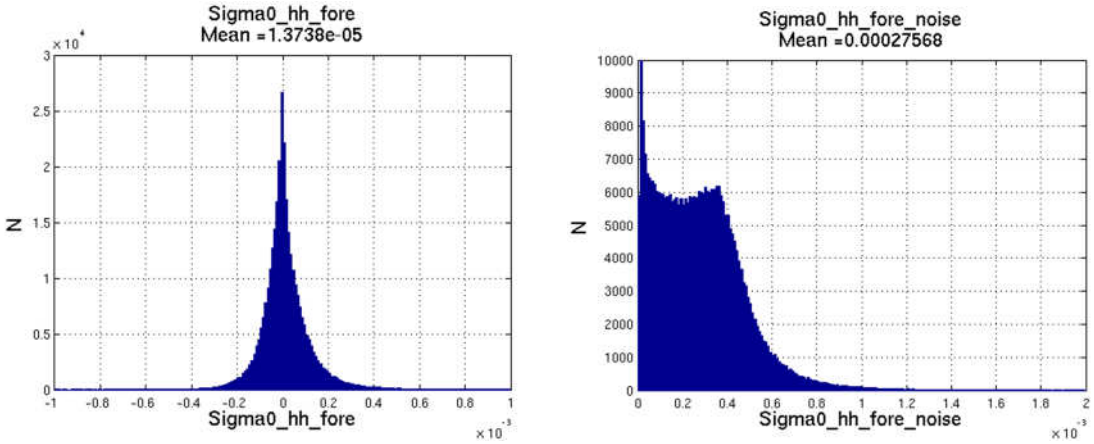

Figure 2-10: Histogram of L1C high-resolution backscatter data in RFI survey mode (no pulse transmission). Left: HH pol with noise-subtracted, Right: HH pol with non-noise subtracted.

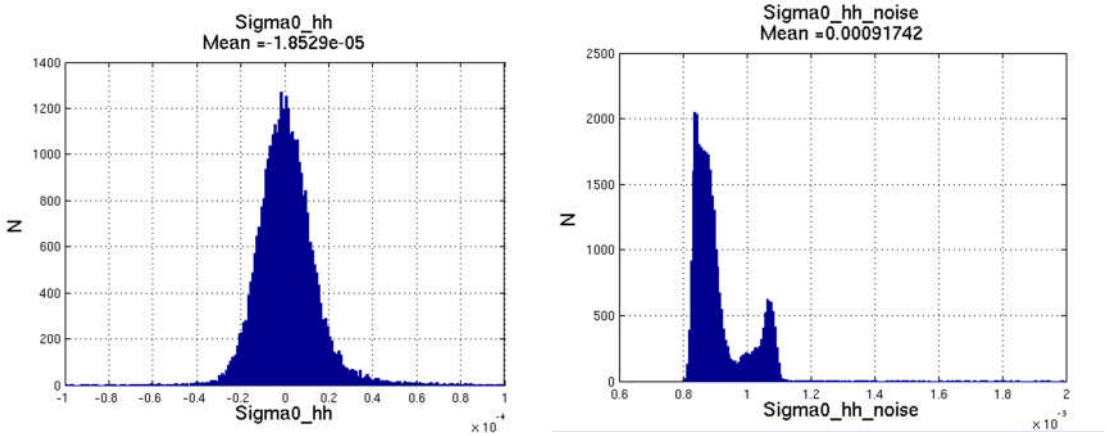

Figure 2-11: Histogram of L1B low-resolution backscatter data in RFI survey mode (no pulse transmission). Left: HH pol with noise-subtracted, Right: HH pol with non-noise subtracted. These data include both land and ocean areas, but no transmission.

Intra-Swath and Inter-Pixel Radiometric Consistency

In this section the process whereby the data are examined for systematic variations as a function of scan angle (azimuth) or as a function of elevation angle within the antenna beam is described. First, the knowledge errors in the instrument pointing were determined. From echo data analysis, it was determined that the instrument pointing required 0.07 degrees of roll and 0.022 degrees of pitch bias adjustment. The look angle adjustment using backscattering from the assumed homogeneous and isotropic Amazon target is also determined (illustrated in Figure 2-12). The nominal look angle is 35.0 degrees and but was adjusted to 34.46. The results below show the backscatter behavior of L1B and L1C backscatter data over the Amazon target as a function of slice number (antenna elevation angle) and scan angle. Figure 2-13 shows the L1B backscatter data, before and after the correction. The backscatter after correction is approximately flat as a function of scan angle and elevation angle (except for the outer slice 12, which is far down on the antenna pattern).

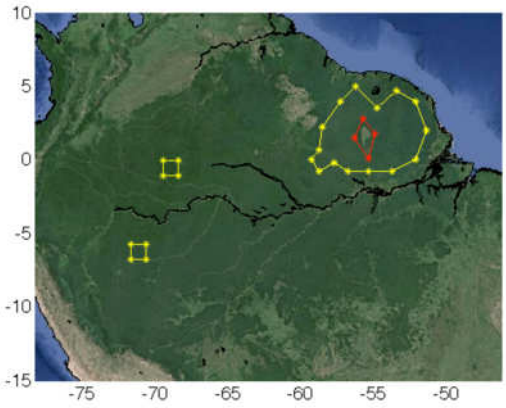

Figure 2-12: Area in the Amazon rainforest used in instrument attitude and look angle analysis. The yellow polygon indicates the region where data are used. The red polygon inside the big yellow polygon is excluded in the analysis.

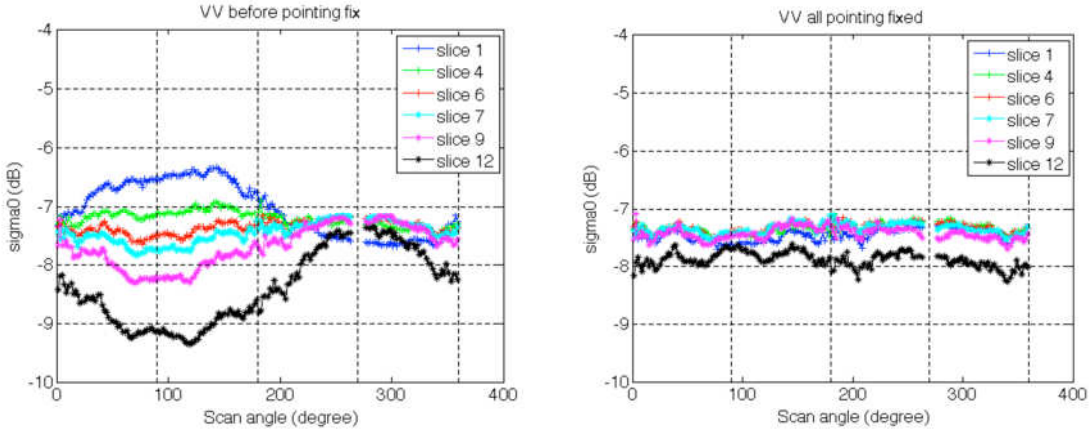

Figure 2-13: L1B radar backscatter from the Amazon target as a function of scan angle and slice number (elevation in antenna beam). This shows improvement after roll, pitch, and look angle biases are applied. Left: before correction, right: after correction. Slice 1 falls at the inner edge of the beam, slices 6 and 7 fall at the center of the beam (zero elevation angle), and slice 12 falls at the outer edge of the beam. Slices near the edges of the beam main lobe are more sensitive to attitude errors because the antenna gain varies more rapidly there as a function of antenna elevation angle.

Similar analysis was performed on L1C high-resolution data. The original results are shown below in Figure 2-14. It was noted that azimuth variation on the order of 1 dB and a nadir anomaly were present; both of which are suspected to be errors in the point spread function area which varies with the geometry of the SAR image.

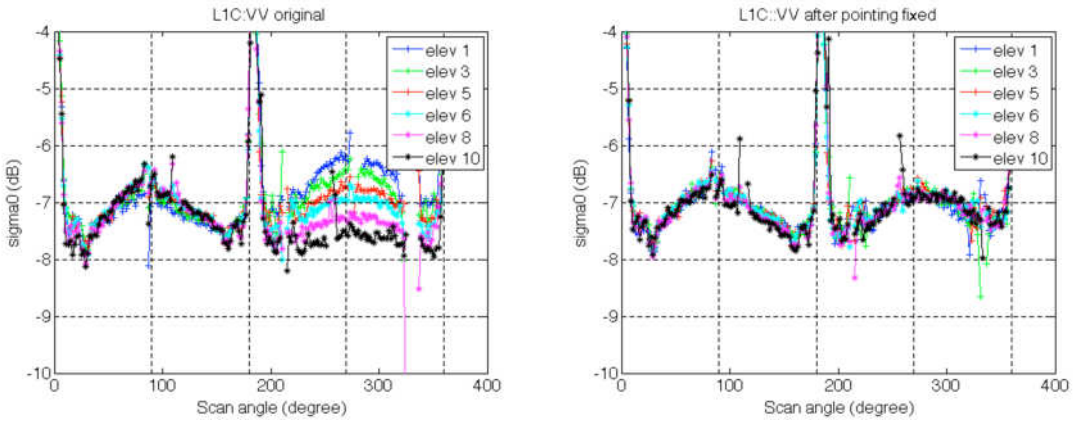

Figure 2-14: L1C radar backscatter from Amazon target as a function of scan angle and elevation bin. Left: before correction, Right: after correction. This shows improvement after roll, pitch, and look angle biases are applied. However, some azimuth variation and nadir region discrepancies remain.

To rectify the azimuth dependent variations for the beta-release, an ad-hoc correction to the backscatter measurements as a function of azimuth (scan) angle was applied. This correction is a temporary stand in for a more accurate approach to be applied in the Validated Release which will calculate the resolution cell area more accurately around the whole conical scan. The effectiveness of the ad hoc correction is checked by taking the ratio of L1C backscatter over L1B backscatter at the same locations over the whole earth. This is done assuming that L1B measurements are fully corrected by the pointing bias corrections and provide reasonable calibrated backscatter. The discrepancies observed in the L1C product are the residual errors due to inaccurate area calculations. The ratio of L1C to L1B is calculated as a function of azimuth angle and orbit fraction. Then, it is averaged over the orbit fraction. The result are shown in Figure 2-15 and indicate that the residual azimuth angle variation is in the order of 0-0.5 dB in co-pol and almost 1.5 dB for cross-pol. A correction is based on this information and it is applied to data. Then, the analysis is performed again on the ad-hoc corrected data. The final result is illustrated in Figure 2-16. It shows that the ad hoc azimuth correction drastically reduce the azimuth variation of the L1C high resolution backscatter data as function of antenna azimuth angle. The nadir anomaly is also reduced in magnitude. Note that, in Figure 2-15 and 2-16, the VH (green lines) are not meaningful because it is the ratio of L1C cross-polarization (HV) to L1B VH.

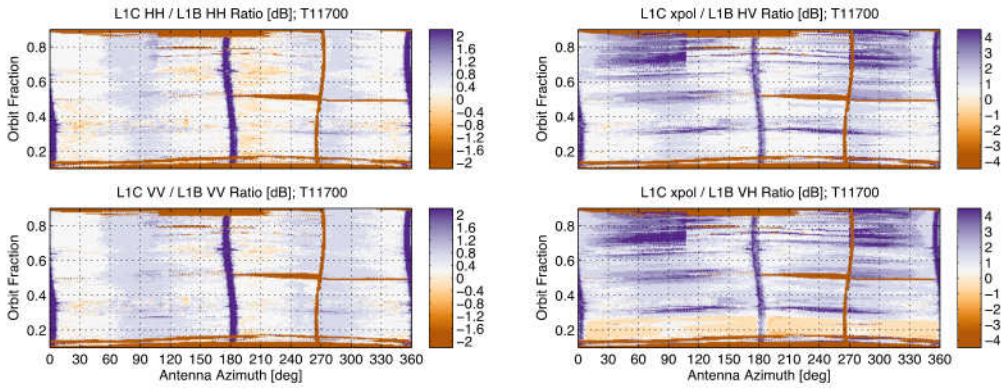

L1C/L1B ratio as a function of antenna azimuth and orbit fraction

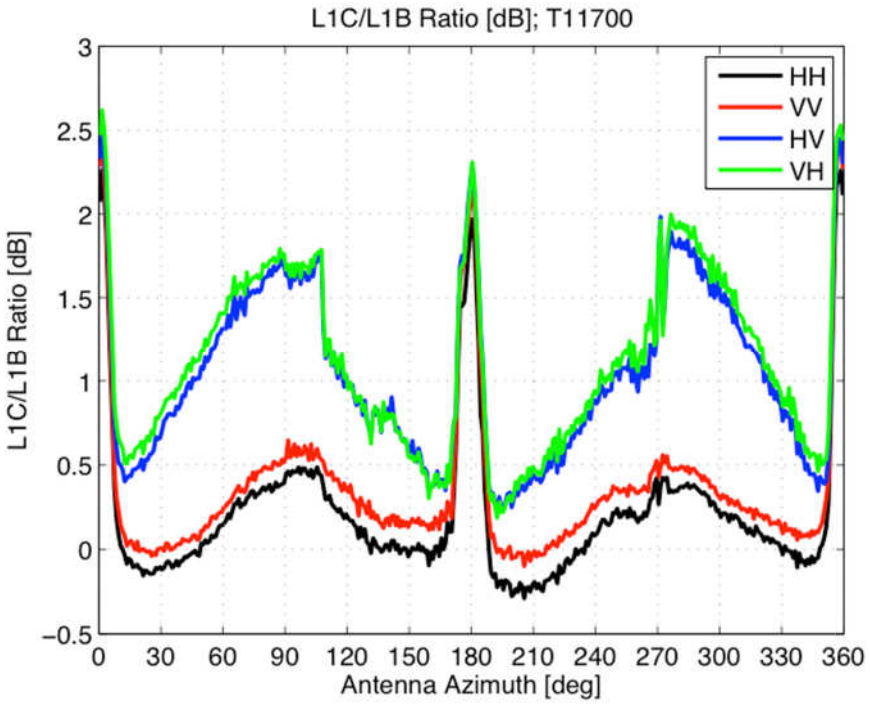

Figure 2-15 : Top: plot of L1C-L1B ration as a function of azimuth angle and orbit fraction, Bottom: plot of L1C-L1B ratio as a function of azimuth angle averaged along the orbit fraction. This is before ad-hoc azimuth angle correction.

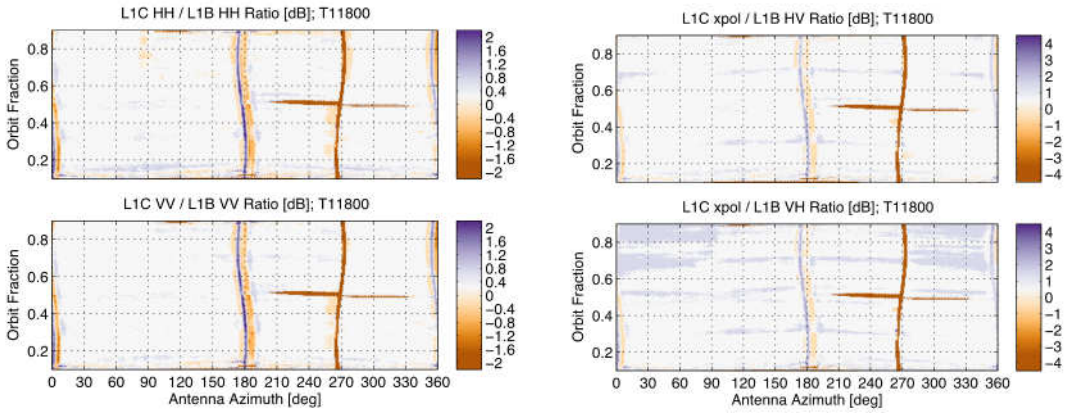

L1C/L1B ratio as a function of antenna azimuth and orbit fraction

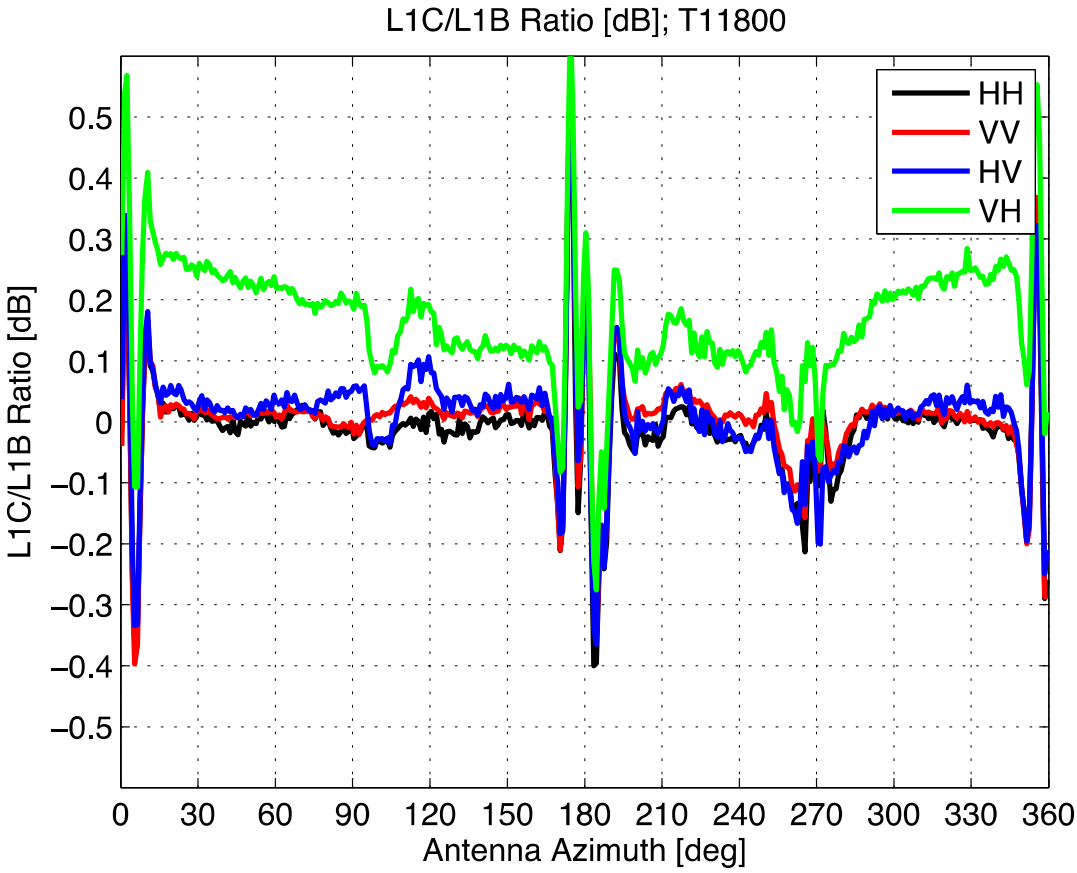

Figure 2-16 : Top: plot of L1C-L1B ration as a function of azimuth angle and orbit fraction, Bottom: plot of L1C-L1B ratio as a function of azimuth angle averaged along the orbit fraction. This is after to the ad-hoc azimuth angle correction is applied.

Radiofrequency Interference Detection and Mitigation

The SAR processor uses a slow-time threshold detection algorithm to identify RFI contaminated samples that are excluded from processing. The detection criterion is based on a median magnitude threshold comparison. Those samples whose magnitude exceed the median magnitude by more than the threshold factor are considered contaminated and discarded. The threshold factor is an adjustable parameter that will be further tuned before the final validated data release. L1C backscatter images with the RFI algorithm OFF and ON are compared in figure 2-17. A location was selected around the Korean peninsula because there are strong RFI signals around that area in the frequency used. The backscatter with RFI algorithm on, off, and the difference is plotted. The difference map shows where the algorithm removed potential RFI contaminated data.

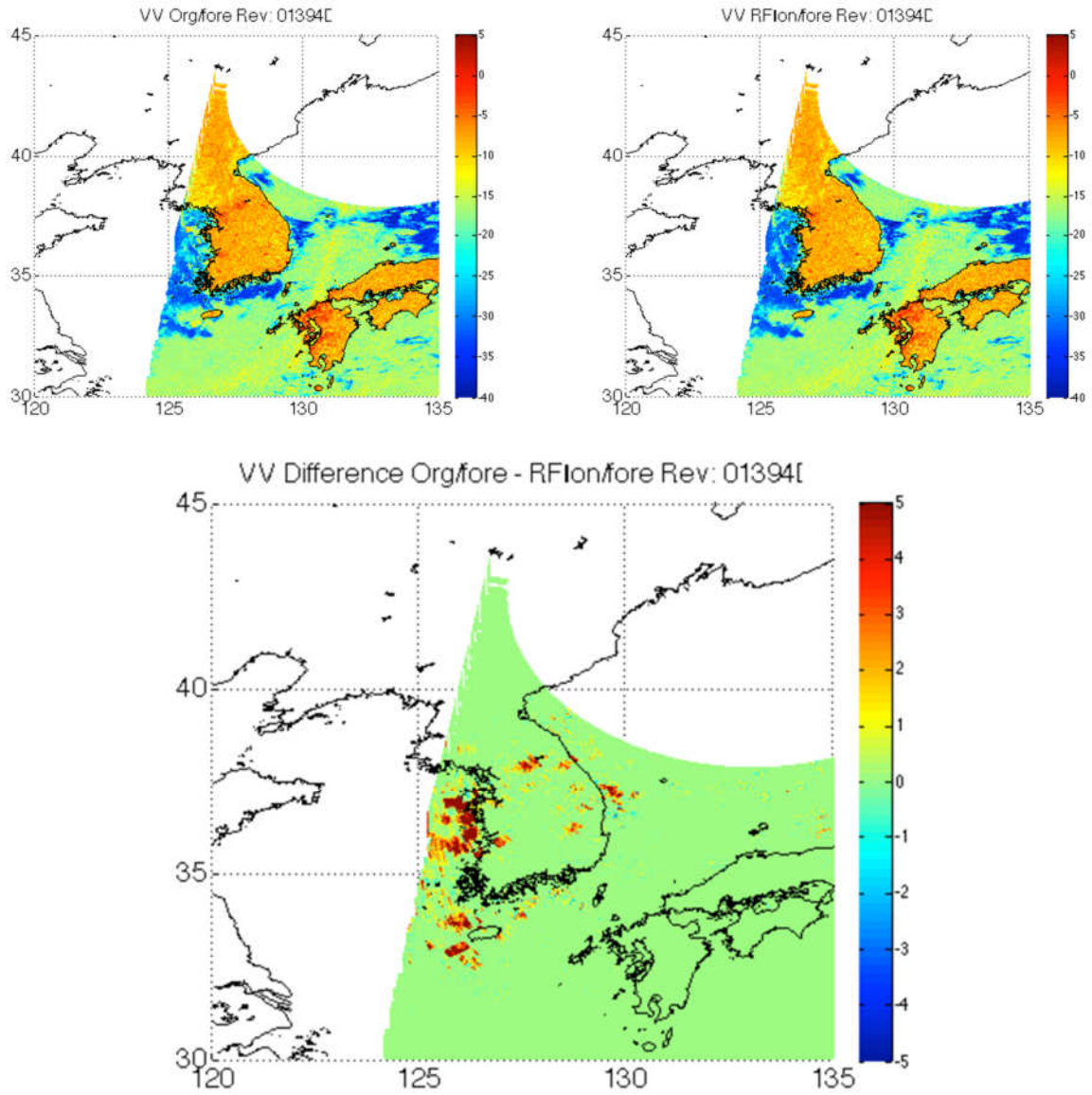

Figure 2-17 : Top row left: plot of backscatter with RFI algorithm OFF, Top row right: plot of backscatter with RFI algorithm ON. Bottom: plot of difference of backscatter with RFI algorithm OFF and ON. This show where and how much sigma0 are corrected with the RFI algorithm.

The tuning of RFI algorithm parameter is performed by adjusting the magnitude-threshold of RFI detection. An initial threshold of 2.0 was used that produced the results above. Optimally, it is desired to set this threshold to be low enough to detect potential RFI but not so low that random noise will trigger unnecessary corrections. To pick the threshold number, the data were processed with the RFI algorithm ON and OFF at a place where little or no RFI was expected. The area around Madagascar was picked and the threshold and process the data were varied with RFI ON and OFF and then the number of pixels affected by the RFI algorithm were compared. The result shows that number of pixels plateau at about 1.8. This means that with lower threshold, there may be an over-detection and over-correction of random noise. On the other hand, with a higher threshold, miss some RFI may be missed, particularly at the place where RFI is more prevalent. For the beta release, the RFI algorithm will be activated with a threshold of 1.8.

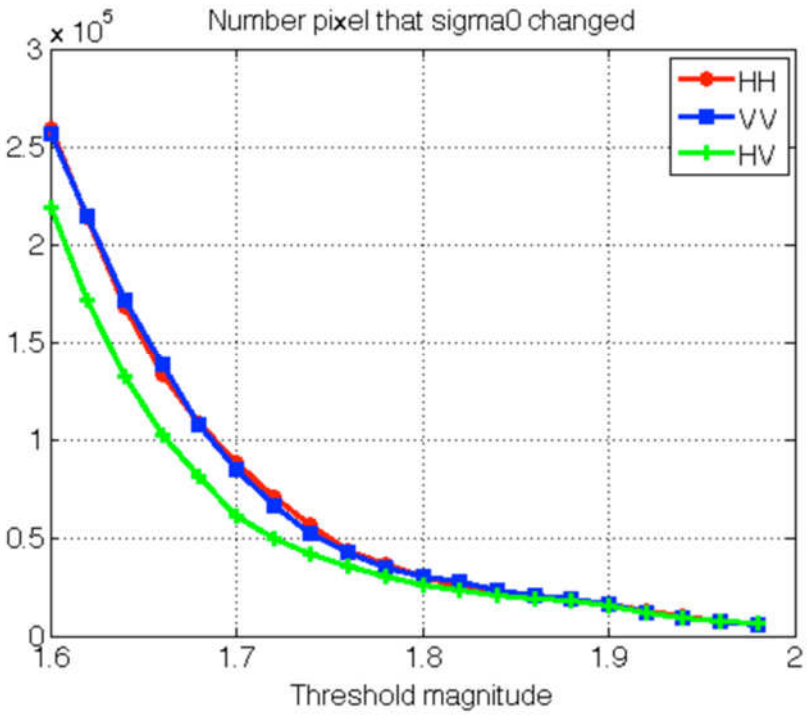

Figure 2-18: Number of pixel affected by RFI algorithm as a function of threshold magnitude used in RFI algorithm. This is performed on data around Madagascar where we expect low RFI presence.

Beta Product Caveats

There are some known issues in the L1 Radar data products in the beta release. These are in the L1C (SAR) radar product. The cross-pol transition flag is always on. In actuality, it should mostly be off. The earth azimuth angles and the earth incidence standard deviation fields in the L1C product are all set to fill values. Faraday rotation corrections are turned off in the SAR processor pending further work, and the reported correction factors in the product should all be 1.0 or fill value. Occasionally, intermediate values are present due to a problem in multi-look averaging across swath grid segment boundaries. These issues and others will be corrected in the final validated product release.

3 Future Work

In three months we expect to have a final validated release of L1 Radar data products that will address some remaining issues. As mentioned above, the beta product shows evidence of systematic errors in the scaling of SAR backscatter measurements as a function of scan angle. This artifact is reduced in magnitude in the beta release using a 1-D ad-hoc correction table. For the final release, we expect to have an improved resolution cell area calculation that will reduce the magnitude of the final ad-hoc table correction. We also plan to implement a multi-dimensional ad-hoc correction table that will permit the expected residual biases as functions of scan angle, elevation angle, and orbit position to be reduced or eliminated. Known issues in the products will be fixed. Work on the Faraday rotation correction in the SAR processor will be completed and activated. Additional analysis of other polarization dependent corrections may lead to some algorithm upgrades in both the low-res L1B processor and the high-res L1C processor. Final tuning of the absolute calibration will use the Amazon and oceans as described above. The science team will decide if an absolute calibration factor needs to be applied to bring results into better agreement with PALSAR and Aquarius.